Analyst

Accepted Manuscript

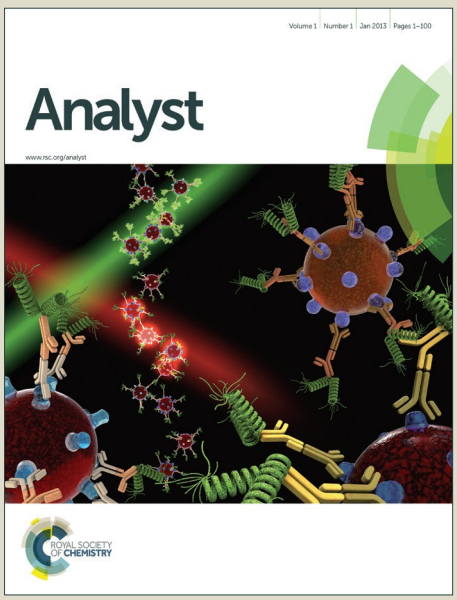

ROYAL SOCIETY OF CHEMISTRY

www.rsc.org/analyst

Electropolymerized phenol derivatives as permselective polymers for biosensor applications

Giammario Calia,[a,b] Patrizia Monti,[c] Salvatore Marceddu,[d] Maria A. Dettori,[c] Davide Fabbri,[c] Samir Jaoua,[e] Robert D. O'Neill,[f] Pier A. Serra,*[b] Giovanna Delogu,[c] and Quirico Migheli[a]

[a] Dipartimento di Agraria and Unità di Ricerca Istituto Nazionale di Biostrutture e Biosistemi, Università degli Studi di Sassari, Viale Italia 39, I-07100 Sassari, Italy.

[b] Dipartimento di Medicina Clinica e Sperimentale, Università degli Studi di Sassari, Viale S. Pietro 43/b, I-07100 Sassari, Italy.

[c] Istituto CNR di Chimica Biomolecolare - UOS Sassari - Traversa La Crucca 3, I-07100, Sassari, Italy.

[d] Istituto CNR di Scienze delle Produzioni Alimentari - UOS Sassari - Traversa La Crucca 3, I-07100, Sassari, Italy.

[e] Department of Biological & Environmental Sciences, College of Arts and Sciences, Qatar University, P.O. Box: 2713, Doha, Qatar.

[f] UCD School of Chemistry and Chemical Biology, University College Dublin, Belfield, Dublin 4, Ireland.

*Corresponding author: E-mail Address: paserra@uniss.it

Amperometric biosensors are often coated with a polymeric permselective film to avoid electroactive interferences by reducing agents present in the target medium. Phenylenediamine and phenol monomers are commonly used to form these permselective films in the design of microsensors and biosensors. This paper aims to evaluate the permselectivity, stability and lifetime of polymers electrosynthesized, using either constant potential amperometry (CPA) or cyclic voltammetry (CV), from naturally occurring phenylpropanoids in monomeric and dimeric forms (eugenol, isoeugenol, dehydrodieugenol and magnolol). Sensors were characterized by scanning electron microscopy and permselectivity analysis. Magnolol formed an electro-deposited polymer with a more defined three-dimensional texture in comparison with the other films. The phenol-derived films showed different permselectivity towards H_2O_2 over ascorbic acid and dopamine, likely to be related with the thickness and the compactness of the polymer. The CV-derived films had a better permselectivity compared to the CPA-corresponding polymers. Based on these results, permselectivity, stability and lifetime of a biosensor for glucose were studied when a magnolol coating was electro-deposited. The structural principles governing the permselectivity of the magnolol-derived film are suggested to be mainly related to the conformational flexibility of this

monomer. Newly designed biosensors, coated with electropolymerized natural phenol derivatives may represent promising analytical devices for different application fields.

Introduction

Over the last 20 years, efforts have been devoted to improve biosensor selectivity and specificity by reducing signals derived from interfering molecules[1]. The global interest on biosensors is increasing significantly in many diverse areas (e.g. health care, industrial process control, military applications, environmental monitoring) with a concomitant need for molecular detection at ever lower concentration limits[2].

Most first-generation enzyme biosensors are based on an oxygen-related electrochemical signal transduction pathway, involving a covalently bonded FAD oxidase (Ox) as the sensitive biological element. An example is the following multi-step oxidation (reactions 1-2) catalyzed by glucose oxidase (GOx):

$$\beta\text{-D-glucose} + \text{GOx/FAD} \rightarrow \text{D-glucono-}\delta\text{-lactone} + \text{GOx/FADH}_2 \quad (1)$$

$$\text{GOx/FADH}_2 + O_2 \rightarrow \text{GOx/FAD} + H_2O_2 \quad (2)$$

The enzyme is usually immobilized onto the surface of a signal transducer (often platinum for electrochemical biosensors), and produces hydrogen peroxide H_2O_2 which is commonly oxidized directly (reaction 3) on the transducer (electrode) surface:

$$H_2O_2 \rightarrow O_2 + 2H^+ + 2e^- \quad (3)$$

In amperometric mode, these biosensors are often characterized by a simple design and fast kinetics (response times of ~1 s are not uncommon[3]) when nanometer thin permselective layers are used, because of the short electron-transfer chain. Unfortunately, the relatively high H_2O_2 oxidation potential necessitates biosensor applied potentials of >0.4 V *vs* Ag/AgCl reference electrode[4], making these devices very sensitive to electrochemical interference species present in the analytical matrix that could compromise their specificity for the substrate. In order to minimize electrochemical interference in complex matrices such as brain extracellular fluid (where ascorbic acid, uric acid, and dopamine and its acid metabolites are among the main interference neurochemicals), permselective polymers may be directly electrosynthesized on the transducer surface [5, 6, 7]. Furthermore for *in-vitro* applications, this approach helps to simplify or eliminate the sample preparation procedure[8,

[9] and allows the direct exposure of the biosensor to the unprocessed matrix material. An alternative approach of electrocatalytic reduction of hydrogen peroxide using, e.g., Prussian Blue shows promise in the design of biosensors, but can suffer from long-term stability issues, especially in neutral media containing sodium ions[10], although these problems can be mitigated by the incorporation of certain surfactants or electrochemical post-treatment procedure[11, 12].

Polyphenylenediamines (PPDs) are commonly used as electro-deposited thin films in the design of microsensors and, as an enzyme-entrapping membrane, in the preparation of biosensors[5, 8, 13]. These polymers form a good permselective barrier on the transducer surface able to ameliorate significantly electroactive interferences by reducing agents present in the target medium[14]. The search for new materials is in progress[2, 7, 15, 16] focusing on improving permselectivity, lifetime of the electrodeposited thin-film and adhesion to the metal surface. The grafting quality of the electrodeposited thin film to the metal surface is a critical feature since only small quantities of enzyme are needed to fabricate a biosensor that can be used repeatedly for measurements. In fact, entrapment of enzymes and proteins on different transducer surfaces is paramount for stability, reproducibility and sensitivity of the biosensor[17].

Alternative polymerized natural compounds would be highly desirable in the packaging of a biosensor where miniaturization, running costs, permselectivity and mass production could be achieved. In addition, to preventing fouling, eliminating interference, controlling the operating regime of the biosensor, the coating materials should be biocompatible since the sample host system must not be contaminated by the biosensor itself. Moreover, the use of biosensors in large areas of health care and food has generated a global interest in the development of safer alternatives to conventional permselective polymers[18].

Besides aromatic diamines, it is acknowledged that thin-films formed by hydroxylated aromatic polymers are highly specific in the detection of small analytes such as hydrogen peroxide, while access of larger molecules is suppressed[19].

2-Methoxyphenols are naturally occurring compounds, that are widely used in the cosmetic and food industries. These compounds and their corresponding dimers are noteworthy for their anti-inflammatory and chemopreventive properties, resulting from antioxidant activity[20]. For example, eugenol, a well-known antioxidant and common food spice, has been electropolymerized on different transductors and its permselective properties toward small solutes of analytical interest (e.g. dopamine, DA) has been studied [21-25].

Often, symmetric dimerization of 2-methoxyphenols, generating hydroxylated biphenyls, enhances their antioxidant activity. Moreover, the higher ability of hydroxylated biphenyls to bind a wide range of proteins compared to other aromatic structures has been demonstrated[26]. Several hydroxylated biphenyls such as magnolol and honokiol, the main constituents of *Magnolia officinalis* are promising pharmacological leads. Magnolol and honokiol have been electropolymerized on different transductors aiming to detect both natural biphenyls with high precision and accuracy[27-31]. Recently, interactions of magnolol with DNA has been studied by electrochemical and spectral methods[32]. Considering the wide interest in naturally occurring compounds as starting monomer to prepare new thin films with improved biosensor properties and acceptable metabolic profiles, we selected some phenols belonging to natural 2-methoxyphenols and hydroxylated biphenyls for further study. In this work the permselectivity and stability of eugenol, isoeugenol, dehydrodieugenol (natural C_2-symmetric dimer of eugenol) and magnolol in the detection of H_2O_2 were evaluated upon electropolymerization by cyclic voltammetry (CV) and constant potential amperometry (CPA) on a Pt/Ir electrode. After electro-deposition, polymeric films were also characterized by scanning electron microscopy (SEM).

Additionally, permselectivity towards H_2O_2, stability and lifetime of a glucose-based biosensor were studied when magnolol-Pt/Ir coating was used as the transducer.

Experimental

Chemicals and solutions

All chemicals were analytical reagent grade or higher purity and dissolved in bidistilled deionized water (MilliQ®). Ascorbic acid, dopamine (DA), hydrogen peroxide (H_2O_2), D-(+)-glucose, glucose oxidase (GOx) from *Aspergillus niger* (EC 1.1.3.4), bovine serum albumin (BSA), *o*-phenylenediamine (*o*PD), glutaraldehyde (GA), dimethyl sulfoxide (DMSO), acetone, eugenol (>98%), ethanol (EtOH, >99.5%), ammonium hydroxide (NH_4OH), sodium hydroxide (NaOH), potassium hexacyanoferrate(III) ($K_3Fe(CN)_6$), hydrochloric acid (HCl) and isoeugenol (*cis-trans* mixture) were purchased from Sigma-Aldrich (Milano, Italy). Magnolol was purchased from Chemos GmbH (Regenstauf, Germany). The naturally occurring compound dehydrodieugenol was synthesized as described in the section 2.2. The phosphate-buffered saline (PBS, 50 mM) solution was prepared using 0.15 M NaCl, 0.04 M NaH_2PO_4 and 0.04 M NaOH from Sigma-Aldrich and then adjusted to pH 7.4. Phosphate buffer (50 mM, pH range 5-8) has been used for studying

the pH effect on permselectivity. GOx solution was prepared by dissolving 180 units of enzyme in 10 µL of PBS and stored at -20 °C. The *o*PD monomer (300 mM for CPA polymerization and 10 mM for CV polymerization) was dissolved in PBS whereas eugenol and isoeugenol (phenol monomers, 10 mM) and magnolol and dehydrodieugenol (phenol dimers, 10 mM) were dissolved in NaOH (100 mM) immediately before use. Stock solutions of DA (100 mM), H_2O_2 (100 mM) and AA (100 mM) were prepared in water immediately before use, while the stock solution of glucose (1 M) was prepared in water 24 hours before use and stored at room temperature. Solutions were kept at 4 °C when not in use. All *in vitro* calibrations were performed using freshly solutions under standard conditions of pressure and temperature. GA (0,1% w/v), and BSA (2% w/v) solutions were prepared in bidistilled water. Teflon-coated platinum (90% Pt, 10% Ir; Ø = 125 µm) and silver wires (Ø = 250 µm) were purchased from Advent Research Materials (Eynsham, England).

Synthesis of dehydrodieugenol

Although dehydrodieugenol is present in natural sources for practical purpose it was prepared according to de Farias Dias[33]. Briefly, the oxidative coupling of 4 g of eugenol (24.36 mM) was carried out in 110 ml 2:1 acetone/water solution alkalinized with 81 mL of an aqueous solution of 25% NH_4OH. After 10 minutes of magnetic stirring, 7.51 g of $K_3Fe(CN)_6$ were dropped in over 4.5 hours, after which another 81 mL of 25% NH_4OH were added. The reaction proceeded at room temperature (25°C) with continuous stirring for 16 hours. Then the solution was acidified with the appropriate quantity of a 10% HCl solution and the precipitate filtered under *vacuum*. The solid was washed with water and then purified by recrystallization from EtOH to achieve dehydrodieugenol in 90% yield as white crystals (mp: 96-8 °C). ^{1}H NMR (CDCl3), δ (ppm): 3.33 (d, J = 6.5 Hz, 4H), 3.79 (s, 6H), 4.96-5.18 (m, 4H), 5.80-6.17 (m, 2H), 6.69 (s, 2H), 6.73 (s, 2H). ^{13}C NMR (CHCl3), δ (ppm): 40.02; 56.02; 110.84;115,59; 123,28; 131.82; 137.79; 141.23; 147.44. See Fig. S5 ESI for ^{1}H and ^{13}C NMR spectra of the synthetized dehydrodieugenol detected in $CDCl_3$ at 399.93 MHz and 100.57 MHz, respectively (Varian Mercury Plus, Palo Alto, USA).

Platinum microsensors and glucose biosensor construction

All the working electrodes were prepared removing the Teflon® insulation from the platinum wires in order to expose 1 mm of bare metal (Fig. 1, Fig. 3, I-J).

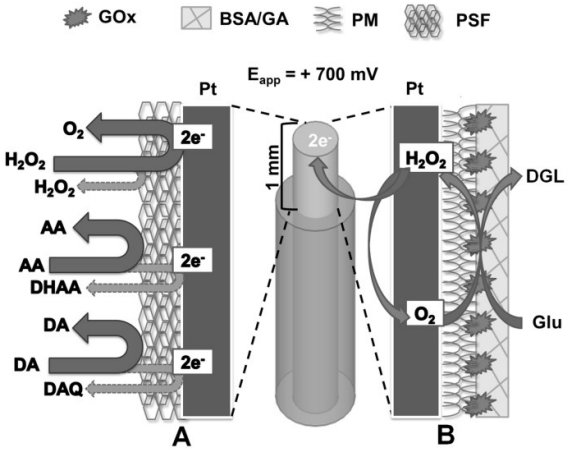

Fig. 1

Electropolymerization and calibration were made using the four-channel equipment (eDAQ QuadStat, e-Corder 410, eDAQ, Australia), Ag/AgCl as reference electrode (RE) and a length of platinum wire (25 mm) as auxiliary electrode (AE). The electro-deposition of the polymeric layers was performed by means of either cyclic voltammetry (CV) or constant potential amperometry (CPA) in 0.1 M NaOH (pH=12.85) containing 10 mM of phenol [23]. *o*PD (10 mM) was dissolved in PBS (pH 7.4) as was described by Killoran and O'Neill[1] (Figure S1, ESI). CV parameters used for each phenol and *o*PD are reported in Table 1.

Table 1

Monomer	Cyclic voltammetry (CV) parameters and oxidation peak potentials						
	Rate (mV/sec)	Lower E_{App} (mV)	Upper E_{App} (mV)	Oxidation peaks (mV ± standard error*) {cycle N}			
				1st	2nd	3rd	4th

1-*o*PD	20	0	+800	+267 ± 7 {1}	-	-	-
2-eugenol	100	0	+2000	+313 ± 2 {1}	+1760 ± 10 {1-5}	-	-
3-*iso*eugenol	100	0	+2000	+74 ± 13 {1}	+1647 ± 13 {1-5}	-	-
4-dehydrodieugenol	100	-300	+2200	+185 ± 4 {1}	+1671 ± 6 {1-5}	+2193 ± 2 {1-5}	-
5-magnolol	100	-300	+2000	+217 ± 13 {1}	+653 ± 5 {2-5}	+1567 ± 3 {1-2}	+1944 ± 7 {1-3}

* standard error of the mean

The CPA was carried out for 15 minutes in the same buffer used for CV; the applied potential for the electropolymerization was fixed at 2 V for phenols (10 mM) and at +0.7 V for *o*PD (300 mM)[1].

Among the microsensors studied, the most promising in terms of H_2O_2 permselectivity was selected as the transducer for glucose biosensor construction (Fig. 1, A). The preparation of the glucose biosensor consisted of dipping (5 times) a working electrode (previously electro-coated with the specific monomer) in a solution of GOx and let it dry for 5 minutes after each dip. The final enzyme-containing net was made by dipping the biosensor in BSA (2%) and GA (0.5 %) solutions to promote the cross-linking and the immobilization of the enzyme (Fig. 1, B).

Microsensor and biosensor *in vitro* characterization

Permselectivity studies were conducted at day 1, 7 and 15 after construction in 20 mL PBS at room temperature. A constant potential of +0.7 V was applied and a calibration was performed after a period of stabilization. The currents generated by different concentrations of DA (50 and 100 μM), H_2O_2 (500 and 1000 μM) and AA (500 and 1000 μM) were recorded for bare Pt electrodes, microsensors (obtained with different phenols) and the glucose biosensor. The pH effect on permselectivity has been studied at day 1 in a pH range comprised between 5 and 8. Considering the pH-related shift of the oxidation peaks (vs Ag/AgCl) and after preliminary CVs on bare Pt for H_2O_2, AA and DA, the applied potentials for CPA analysis were corrected for each pH point (5, 6, 7 and 8). Calibration with glucose

was performed on glucose biosensor in order to investigate biosensor performance (K_M, V_{MAX}, linear region slope, AA blocking, LOD and LOQ). Separate group of sensors were used for scanning electron microscopy (SEM) studies at day 1 and 15 after polymerization to evaluate the aging-related surface changes.

Statistical analysis

DA, H_2O_2 and AA concentrations were expressed in μM while glucose concentrations were given as mM. Oxidation currents were expressed in nanoampere (nA) and given as baseline-subtracted values ± standard error of the mean. The AA ΔI value represents the difference between the current resulting from the injection of 1 mM and 0.5 mM of AA in the electrochemical cell[34]. The percent permselectivity (S%), Eqs. (1) and (2) of H_2O_2 *versus* AA (AA/H_2O_2 S%) or DA (DA/ H_2O_2 S%) was calculated after calibrations by using the following equations[35]:

$$(\text{AA/HP})\ \text{S\%} = \frac{\text{I AA (1 mM) at Pt/polymer}}{\text{I H}_2\text{O}_2\text{(1 mM) at Pt/polymer}} \times 100 \quad (1)$$

$$(\text{DA/HP})\ \text{S\%} = \frac{\text{I DA (1 mM) at Pt/polymer}}{\text{I H}_2\text{O}_2\text{(1 mM) at Pt/polymer}} \times 100 \quad (2)$$

The limit of detection [LOD, Eq. (3)] and limit of quantification [LOQ, Eq. (4)] were determined using a statistical method based on the standard deviation (σ) of the response and the linear region slope (LRS) of the calibration curve according to Rocchitta et al.[17]:

$$\text{LOD} = 3.3\sigma/\text{LRS} \quad (3)$$

$$\text{LOQ} = 10\sigma/\text{LRS} \quad (4)$$

Statistical significance ($p < 0.05$) between groups was evaluated by calculating unpaired t-test, while differences within groups were evaluated by paired t-test.

Results and discussion

CV and CPA electrosynthesis of polymeric films

Polymeric films were electro-deposited by means of CV or CPA. Cyclic voltammograms illustrate the redox processes on Pt-Ir surface of the four phenols used in this study (eugenol, isoeugenol, dehydrodieugenol and magnolol) (Fig. 2).

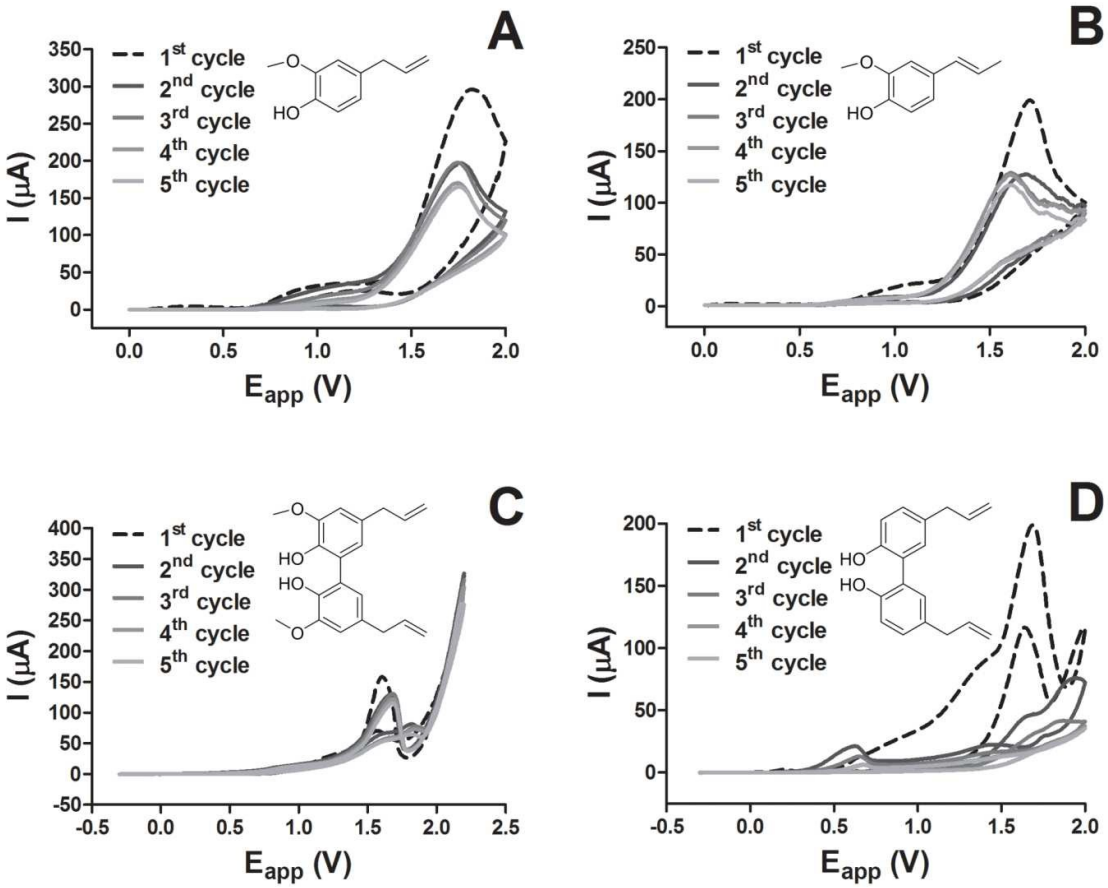

Fig. 2

The oxidation peaks are indicated in Table 1.

In phenol structures, the first oxidation potential was found to vary in the range of 74 to 312 mV, depending on structural effects. Also *o*PD monomer was studied (as a reference molecule) and its cyclic voltammograms are reported in Fig. S1 (ESI). The CV parameters (Table 1) were set based on the existing literature for *o*PD[1] and eugenol[23] while they were obtained experimentally for magnolol and the other phenols. The cycle-by-cycle reduction in the amplitude of the oxidation peaks, visible in the voltammograms of all the studied molecules, is indicative of the formation of non-conductive polymers. Different CV shapes

have been observed among monomer and dimer phenols affecting polymerization on the electrode surface likely due to a lower phenolic O-H bond dissociation enthalpy of dimer respect to monomer[36, 37]. Magnolol adsorbed on the electrode surface with the highest decrease of oxidation peak current on the second potential sweep, while, after the third potential sweep, the oxidation peak current was stable. Dehydrodieugenol formed a non-conductive polymer very rapidly, probably due to a better stabilization of the radical in dehydrodieugenol than in the magnolol structure. This is in accordance with the observed higher antioxidant activity of dehydrodieugenol compared to magnolol[38, 39]. The presence of two methoxyl groups in the phenol ring (guaiacyl unit) of dehydrodieugenol have a positive influence on the formation and lifetime, through a stabilization effect (weak π-donor), of the corresponding phenoxyl radical. Eugenol and isoeugenol have comparable CV profiles, although the oxidation peak of isoeugenol is better shaped, confirming the different radical species described for these monomers[40]. Isoeugenol forms a reactive quinone methide radical likely responsible for the lowest first oxidation potential detected in the phenols studied, whereas phenoxyl/orthoquinone radical have been estimated for eugenol. The large wave shape observed for eugenol could also be due to a higher superimposition of the peaks generated from both free and adsorbed forms. The different shape of CV spectra of eugenol and dehydrodieugenol would exclude coupling reaction of eugenol radical in solution, thus polymerization occurs preferentially on the electrode surface. In general, the ability of phenols to form the phenoxyl radical and the stability of the radical species generated according to the phenol structure[41], influenced the degree of electropolymerization in the CV assays.

As seen in literature[23], the upper limit of a potential sweep used to deposit the polymer by cyclic voltammetry influences the permselectivity of a polyeugenol film. Negative charges formation observed applying high potentials can reject interference molecules bearing anionic charge, such as AA. Nevertheless, polyeugenol film for sensor application has been electropolymerized by mean of CV at lower potential[24]. In the present work the CPA electropolymerization (e-poly) has been carried out by setting the oxidation potential for each molecule on the basis of that previously reported and our present CV results (see paragraph 2.3). Pivotal experiments, that are in progress in our laboratory, suggest that low polymerization potentials (ranging from 150 mV until 700 mV *vs* SCE) improve permselectivity of a CPA-poly-eugenol film (data not shown).

Exponential decay of the oxidation currents were observed during the entire period of the e-poly (data not shown) indicating, also in this case, the formation of non-conductive films on the surface of the Pt-Ir electrodes.

SEM study of polymeric films at day 1

SEM microphotographs illustrate the surface of the permselective sensors at day 1 (Figure 3).

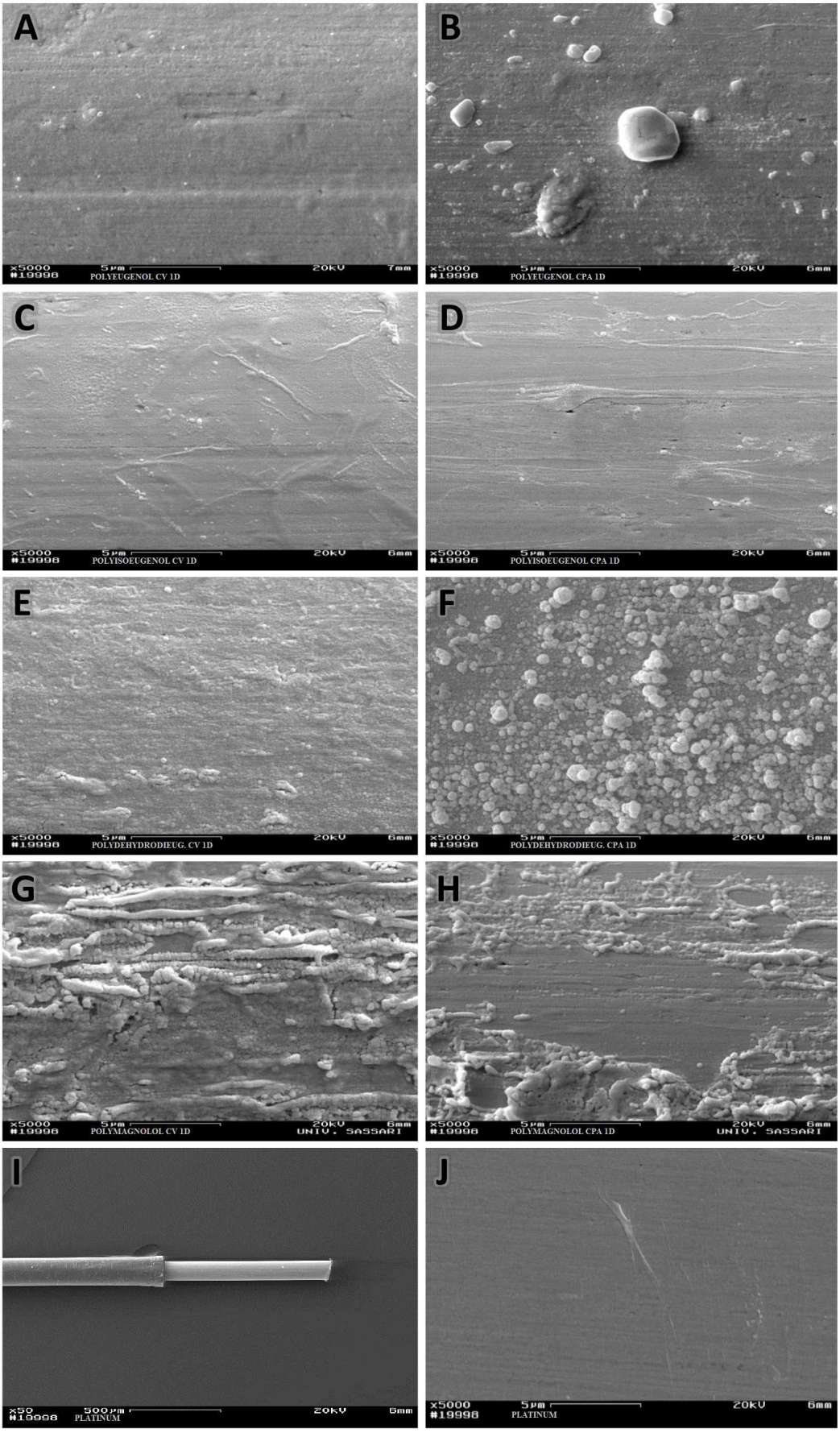

291

Fig. 3

Poly-eugenol (Fig. 3, A-B) and poly-isoeugenol (Fig. 3, C-D), electro-deposited by CV and CPA, respectively, exhibited a smooth and compact surface, while poly-dehydrodieugenol (Fig. 3, E-F) showed a rough and granular surface particularly upon CPA electrodeposition (Fig. 3, F). The different behavior of electrodeposition might be due to the limited area available for orientation of hindered phenols on electrode surface like dehydrodieugenol that limit the control of polymerization. It is acknowledged that Pt electrode absorption of eugenol involves the allyl chain[23]. Magnolol, structurally similar to dehydrodieugenol and eugenol but lacking in the guaiacyl moiety, is conformationally more flexible allowing the generated conformer radicals to be oriented in the electrode surface in an easier manner. Magnolol formed a electropolymer with a more defined three-dimensional texture in comparison with the other films (Fig. 3, G-H). In particular, the CV-obtained film was characterized by the formation of longitudinal ridges (Fig. 3, G) while CPA electro-synthesis resulted in the formation of a composite pattern in which smooth regions alternate with rough zones (Fig. 3, H). Also the poly-*o*PD (PPD) film was characterized by SEM (Fig. S2, ESI) and resulted in a quite compact and smooth surface, confirming previous observations[1].

Sensors sensitivity and selectivity studies at day 1

Table 2 summarizes the results concerning the electrochemical studies performed on day 1 on the new polymers in comparison with PPD (widely used biosensor permselective polymer) (Table 2).

Table 2

Design of Pt/Ir cylinder coated with permselective film	*In vitro* electrochemical characterisation at Day 1					
	Linear regression		Limit of detection and quantification		Permselectivity	
	LRS (nA μM^{-1})	R^2	LOD (μmol l^{-1})	LOQ (μmol l^{-1})	AA/H_20_2 (S%)	DA/H_20_2 (S%)

1-Pt_c/PPD	CV	0.97 ± 0.01	0.999	0.06 ± 0.01	0.19 ± 0.02	6.11 ± 0.55	9.03 ± 0.87
	CPA	0.63 ± 0.01	0.992	0.07 ± 0.06	0.22 ± 0.02	0.16 ± 0.02	9.78 ± 1.01
2-Pt_c/polyeugenol	CV	0.26 ± 0.01	0.999	0.28 ± 0.03	0.86 ± 0.08	1.42 ± 0.15	13.04 ± 1.12
	CPA	0.32 ± 0.01	0.999	0.18 ± 0.02	0.54 ± 0.06	7.58 ± 0.70	24.03 ± 2.20
3-Pt_c/poly*iso*eugenol	CV	0.22 ± 0.01	0.998	0.19 ± 0.02	0.58 ± 0.06	4.81 ± 0.50	33.10 ± 2.99
	CPA	0.15 ± 0.01	0.996	0.26 ± 0.03	0.80 ± 0.08	145 ± 15	65.57 ± 7.02
4-Pt_c/poly dehydrodieugenol	CV	0.29 ± 0.01	0.999	0.17 ± 0.02	0.52 ± 0.05	7.56 ± 0.70	18.10 ± 1.67
	CPA	0.41 ± 0.02	0.992	0.13 ± 0.01	0.38 ± 0.04	26.17 ± 2.44	19.95 ± 2.12
5-Pt_c/polymagnolol	CV	0.08 ± 0.01	0.998	0.58 ± 0.05	1.76 ± 0.15	0.99 ± 0.08	4.53 ± 0.40
	CPA	0.41 ± 0.01	0.994	0.12 ± 0.01	0.35 ± 0.04	51.1 ± 5.0	16.0 ± 1.5

The parameters investigated were: H_2O_2 linear slope (0-1 mM), LOD, LOQ and AA/H_2O_2 and DA/H_2O_2 permselectivity. PPD obtained by CV exhibited the highest H_2O_2 sensitivity (0.97 ± 0.01 nA μM^{-1}) while after CPA e-poly the sensitivity was 35% lower (0.63 ± 0.01 nA μM^{-1}). The phenol-derived films showed different H_2O_2 permeabilities, likely to be related with the thickness and the compactness of the polymer; in particular CPA-obtained polydehydrodieugenol, polymagnolol, polyeugenol and poly*iso*eugenol sensors showed good H_2O_2 sensitivitiy (0.41 ± 0.02 nA μM^{-1}, 0.41 ± 0.01 nA μM^{-1}, 0.32 ± 0.01 nA μM^{-1} and 0.15 ± 0.01 nA μM^{-1}, respectively) while CV-electrosynthetized films resulted in poor

H_2O_2 sensitivity, ranging from 0.29 ± 0.01 nA μM^{-1} (poly-dehydrodieugenol) to 0.08 ± 0.01 nA μM^{-1} (polymagnolol). All the studied polymers showed a good hydrogen peroxide linearity with R^2 comprised between 0.992 and 0.999.

H_2O_2 LOD and LOQ analysis showed that, also in this case, PPD is the best polymer with a sensor LOD of 0.06 ± 0.01 $\mu M\ l^{-1}$ and a LOQ of 0.19 ± 0.02 $\mu M\ l^{-1}$ after CV electrosynthesis (similar results were obtained after CPA). CV obtained films resulted in a lower sensor LOD and LOQ compared to the corresponding CPA-electrosynthetized polymers; in particular CPA-polymagnolol exhibited a LOD of 0.12 ± 0.01 $\mu M\ l^{-1}$ and a LOQ of 0.35 ± 0.04 $\mu M\ l^{-1}$; these values were similar in the other polymers except for poly-isoeugenol with higher LOD and LOQ under CV polymerization (Table 2). AA/H_2O_2 and DA/H_2O_2 percent permselectivities (AA/H_2O_2 S% and DA/H_2O_2 S%) were calculated as previously described (paragraph 2.5) by injecting in the electrochemical cell H_2O_2 (1 mM), AA (1 mM) or dopamine (0.1 mM). CPA-PPD showed a AA/H_2O_2 S% of 0.16 ± 0.02 and DA/H_2O_2 S% of 9.78 ± 1.01. CV-polymagnolol exhibited very good values of permselectivty (AA/H_2O_2 S% = 0.99 ± 0.08 and DA/H_2O_2 S% = 4.53 ± 0.40) while CV- poly-eugenol presented a AA/H_2O_2 S% of 1.42 ± 0.15 and DA/H_2O_2 S% of 13.04 ± 1.12. All CPA-derived phenolic polymers exhibited very poor permselective properties (Table 2). In general, all the CV-derived films had a better S% compared to the CPA-corresponding polymers except for PPD.

During calibrations conducted in different pH phosphate buffers (range 5-8) permselectivity changes did not occurred for the studied polymers with the only exception of CV-poly*iso*eugenol: the increase of pH resulted in a decrease of AA/H_2O_2 S% (-1.71 ± 0.21 AA/H_2O_2 S% • pH^{-1}; $R^2 = 0.97$) and in a concomitant increase of DA/H_2O_2 S% (9.95 ± 0.75 DA/H_2O_2 S% • pH^{-1}; $R^2 = 0.99$). The two trends (see Fig. S6, ESI) resulted inversely related with a Pearson correlation coefficient (r) equal to -0.998 and a p value of 0.002 ($R^2 = 0.99$).

Since the H_2O_2 detection on bare Pt was uninfluenced by pH changes (data not shown), and the dissociation grade of AA and DA is the same for all studied films (for each pH value), the described phenomenon seems to be related to the polyisoeugenol film. As previously reported[40], isoeugenol is the only monomer that forms a reactive quinone-methide radical. This particular electropolymerisation mechanism could be responsible of the observed behaviour suggesting pH-dependent ion-exchange properties. Further studies are necessary to validate this hypothesis.

Aging studies on the permselectivity of polymeric films

Fig. S3 (ESI) summarizes the results from electrochemical studies with the new polymers compared to the standard PPD after 15 days. The studied parameters are linear region slope and permselectivity (S%). Both CPA-PPD and CV-PPD showed an excellent H_2O_2 slope; under the first condition (CPA-PPD), H_2O_2 slope was relatively constant (0.63 ± 0.01 nA μM^{-1} on day 1 *vs* 0.69 ± 0.04 nA μM^{-1} on day 15), whereas in CV-PPD there was a 40% decrease (from 0.97 ± 0.01 nA μM^{-1} on day 1 to 0.59 ± 0.02 nA μM^{-1} on day 15 $p<0.05$). The permselectivity (AA/H_2O_2 S% and DA/H_2O_2 S%) was calculated as described previously on day 1, 7 and 15. The ratio AA/H_2O_2 S% of CPA-PPD was 0.16 ± 0.02 on day 1, whereas it was 0.24 ± 0.02 on day 15 DA/H_2O_2 S% decreased by almost 9 times from 9.78 ± 1.01 on day 1 to 1.10 ± 0.12 on day 15 ($p<0.05$). For CV-PPD values of AA/H_2O_2 S% of 6.11 ± 0.55 on day 1 *vs* 2.92 ± 0.31 on day 15 were observed ($p<0.05$); the DA/H_2O_2 S% value was constant, (9.03 ± 1.01 on day 1 and 7.97 ± 0.82 on day 15). SEM images taken on day 1 and on day 15 (Fig. S2; ESI) confirm PPD as a compact and smooth polymer, with small craters, as observed previously after both CV and CPA electropolymerization.

Polymeric films derived from phenols displayed different permeability towards H_2O_2, probably depending on the thickness and compactness of the polymer. Each phenol was oxidized and polymerized on the electrode surface soon after the reaction started and the electrode became coated with the oxidized film. CPA-polydehydrodieugenol, poly-magnolol, polyeugenol and poly*iso*eugenol microsensors were sensitive towards H_2O_2 on day 1 (Table 2 and paragraph 3.3), but displayed a linear region slope decrease over time ($p<0.05$ *vs* day 1). Polymeric films electrosynthetized in CV have demonstrated a low sensitivity to H_2O_2 already on day 1 (Table 2), confirming the same trend on day 7 and on day 15 ($p<0.05$ *vs* day 1). Only CV-poly-magnolol microsensors maintained a constant slope up to day 7 increasing in sensitivity at day 15 (30% increase from day 1 ($p<0.05$).

Fig. S3 (ESI) illustrates the excellent permselective properties of CV-polymagnolol already on day 1 (Table 2), day 7 (AA/H_2O_2 S% = 1.36 ± 0.12 and DA/H_2O_2 S% = 3.56 ± 0.40) and day 15 (AA/H_2O_2 S% = 1.57 ± 0.11 and DA/H_2O_2 S% = 4.57 ± 0.60).

Also the CV-polyeugenol, compared to other polymers, maintained an excellent permselectivity on day 7 (AA/H_2O_2 S% = 2.17 ± 0.20 and DA/H_2O_2 S% = 7.31 ± 0.70) and on day 15 (AA/H_2O_2 S% = 0.79 ± 0.08 and DA/H_2O_2 S% = 4.31 ± 0.40).

All the new polymers electrosynthesized by CPA showed a low permselectivity from day 1 through day 15. The CPA-polyeugenol, while showing an improvement of the AA/H_2O_2 S% value from day 1 (AA/H_2O_2 S% = 7.58 ± 0.70) to day 15 (AA/H_2O_2 S% = 0.42 ± 0.04),

displayed high S% values for dopamine from day 1 (DA/HP S% = 24.03 ± 2.20) to day 15 (DA/H_2O_2 S% = 13.59 ± 1.34).

SEM analyses (Fig. S4, ESI) did not provide evidence for any structural change in the new polymers after 15 days.

Polymeric films obtained in CV presented a better S% compared to the corresponding polymers electrosynthetized in CPA, with the only exception of CPA-PPD.

Glucose biosensor characterization

Based on the electrochemical results, a glucose biosensor was constructed with poly-magnolol electrosynthesized by CV. *In vitro* sensitivity of the glucose biosensor (Fig. 4) has been determined by injecting in the electrochemical cell known amounts of glucose (ranging from 0 to 140 mM) (Fig. 4).

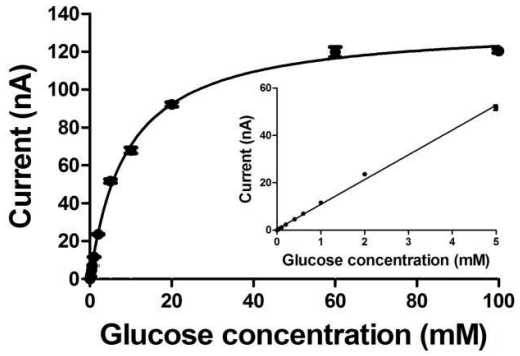

Fig. 4

The calibration curve shows a classical Michaelis-Menten kinetics, with R^2= 0.997 (n = 3), V_{max} and K_M = 134 ± 5 nA and 9.03 ± 0.81 mM, respectively. The linear region slope was evaluated by considering concentrations included between 0 and 5 mM, with R^2 = 0.997 (n = 3) and a slope at 10.46 ± 0.19 nA mM^{-1}. LOD and LOQ values were 4.3 ± 0.4 µM L^{-1} and 13 ± 2 µM L^{-1}, respectively. To evaluate the shielding effect of polymagnolol towards potentially interfering molecules such as ascorbic acid (AA) and dopamine (DA), two distinct calibrations were carried out: the first one with AA (within a 0 - 1000 µM range), and the second one with DA (0 - 100 µM range). Based on these calibrations, two values were calculated: ΔI AA = -0.13 nA, representing the difference between the current produced by injection of 1 mM AA and the current produced by 0.5 mM AA; and ΔI DA =

5.39 nA, representing the difference between the current generated by injection of 100 μM and 50 μM DA. The aging studies on the glucose biosensor (data not shown) showed H_2O_2 sensitivity and permselectivity similar to the microsensors prepared with CV-poly-magnolol, and previously described.

Conclusions

A small collection of polymeric films derived from compounds belonging to natural 2-methoxy phenols and hydroxylated biphenyls was synthesized in the present study by using two electrosynthesis protocols. Structural features of the phenols were found to influence their reactivity in the formation of the film and some general trends has been observed.

The structural principles governing the permselectivity of the magnolol-derived film are supposed to be in relationship with the conformational flexibility of magnolol rather than the resonance-effective guaiacyl unit common to the other phenols. By virtue of the biphenylic structure of magnolol, a better interaction with the enzyme is possible compared to the phenol monomers. The final effect would be a stronger grafting of the enzyme to the electropolymerized thin film.

The electrodes coated with phenols both in CV and CPA are stable and responsive. They are still functional and may be used even though they do not longer meet the starting electrode specifications. Taking into account the known electrochemical behavior of natural phenols[42, 43], sustainable coatings that may represent an effective alternative to PPD can be designed.

Acknowledgements

This publication was made possible by NPRP grant # NPRP 4 - 259 - 2 – 083 from the Qatar National Research Fund (a member of Qatar Foundation). The statements made herein are solely the responsibility of the authors.

Electronic Supplementary Information

Electronic Supplementary Information (ESI) are available for this paper.

Notes and references

1 S.J. Killoran and R.D. O'Neill, *Electrochim. Acta*, 2008, **53**, 7303-7312.

2 J. Tian, Q. Liu, A.M. Asiri, A.H. Qusti, A.O. Al-Youbi and X. Sun, *Nanoscale*, 2013, **5**, 11604-11609.

3 R.D. O'Neill, J.P. Lowry, G. Rocchitta, C.P. McMahon and P.A. Serra, *Trends Anal. Chem.*, 2008, **27**, 78–88.

4 Y.Q. Dai and K.K. Shiu, *Electroanalysis*, 2004, ***16***, 1806–1813.

5 G. Rocchitta, O. Secchi, M.D. Alvau, D. Farina, G. Bazzu, G. Calia, R. Migheli, M.S. Desole, R.D. O'Neill and P.A. Serra, *Anal. Chem.*, 2013, ***85***, 10282-10288.

6 S. Vaddiraju, D.J. Burgess, F.C. Jain and F. Papadimitrakopoulos, *Biosens. Bioelectron.*, 2009, ***24***, 1557-1562.

7 H. Matsuhisa, M. Tsuchiya and Y. Hasebe, *Colloids Surf. B Biointerfaces*, 2013, **111**, 523-529.

8 G. Calia, G. Rocchitta, R. Migheli, G. Puggioni, Y. Spissu, G. Bazzu, V. Mazzarello, J.P. Lowry, R.D. O'Neill, M.S. Desole and P.A. Serra, *Sensors (Basel)*, 2009, **9**, 2511-2523.

9 A. Rasooly and K.E. Herold, *J. AOAC Int.*, 2006, **89**, 873-883.

10 P. Salazar, M. Martin, R. Roche, J.L. Gonzalez-Mora, and R.D. O'Neill, *Biosens. Bioelectron.*, 2010, **26**, 748–753.

11 P. Salazar, M. Martin, R.D. O'Neill, R. Roche and J.L. Gonzalez-Mora, *J. Electroanal. Chem.*, 2012, **674**, 48–56.

12 Z. Wang, H. Yang, B. Gao, Y. Tong, X. Zhang, L. Su, *Analyst,* 2014, **139**, 1127-1133.

13 X. Jing-Juan and C. Hong-Yuan, *Anal. Biochem.*, 2000, **280**, 221-226.

14 S.A. Rothwell, M.E. Kinsella, Z.M. Zain, P.A. Serra, G. Rocchitta, J.P. Lowry and R.D. O'Neill, *Anal. Chem.*, 2009, **81**, 3911-3918.

15 Y.L. Yang, T.F. Tseng and S.L. Lou, *Conf. Proc. IEEE Eng. Med. Biol. Soc.*, 2007, 6625-6628.

16 (15) M. Ma, Z. Miao, D. Zhang, X. Du, Y. Zhang, C. Zhang, J. Lin, Q. Chen, *Biosens. Bioelectron*., 2015, **64**, 477-484s.

17 G. Rocchitta, O. Secchi, M.D. Alvau, R. Migheli, G. Calia, G. Bazzu, D. Farina, M.S. Desole, R.D. O'Neill and P.A. Serra, *Anal. Chem.*, 2012, **84**, 7072-7079.

18 Y. Oztekin, Z. Yazicigil , A. Ramanaviciene, A. Ramanavicius, *Sensor Actuat. B-Chem.* 2011, **152**, 37-48.

19 G. Milczarek and A. Ciszewski, *Electroanalysis*, 2003, **15**, 529-532.

20 S. Fujisawa, T. Atsumi, Y. Murakami and Y. Kadoma, *Arch. Immunol. Ther. Exp. (Warsz)*, 2005, **53**, 28-38.

21 B.A. Patel, M. Arundell, K.H. Parker, M.S. Yeoman and D. O'Hare, *Anal. Chem.*, 2006, **78**, 7643-7648.

22 G. Milczarek and A. Ciszewski, *Electroanalysis*, 1998, **10**, 791-793.

23 A. Ciszewski and G. Milczarek, *Electroanalysis*, 2001, **13**, 860-867.

24 R. Toniolo, N. Dossi, A. Pizzariello, S. Susmel and G. Bontempelli, *Electroanalysis*, 2011, **23**, 628-636.

25 G. Milczarek and A. Ciszewski, *Colloids Surf. B Biointerfaces*, 2012, **90**, 53-57.

26 P.J. Hajduk, M. Bures, J. Praestgaard and S.W. Fesik, *J. Med. Chem.*, 2000, **43**, 3443-3447.

27 T. Liu, X. Zheng, W. Huang and K. Wu, *Colloids Surf. B Biointerfaces*, 2008, **65**, 226-229.

28 X. Yao, X. Xu, P. Yang and G. Chen, *Electrophoresis*, 2006, **27**, 3233-3242.

29 X. Yang, M. Gao, H. Hu, and H. Zhang, *Phytochem. Anal.*, 2011, **22**, 291-295.

30 W. Huang, T. Gan, S. Luo and S. Zhang, *Ionics*, 2013, **19**, 1303-1307.

31 J. Zhao, W. Huang and X. Zheng, *J. Appl. Electrochem.*, 2009, **39**, 2415-2419.

32 C. Zhou, Y. Dong, Z. Li, X. Xu and Z. Liu, *J. Electroanal. Chem.*, 2010, **642**, 115-119.

33 A. De Farias Dias, *Phytochemistry*, 1988, **27**, 3008-3009.

34 M.R. Ryan, J.P. Lowry and R.D. O'Neill, *Analyst*, 1997, **112**, 1419-1424.

35 S.A. Rothwell and R.D. O'Neill, *Phys. Chem. Chem. Phys.,* 2011, **13**, 5413-5421.

36 Y. Kadoma, S. Ito, I. Yokoe and S. Fujisawa, *In Vivo*, 2008, **22**, 289-296.

37 Y. Murakami, A. Kawata, Y. Seki, T. Koh, K. Yuhara, T. Maruyama, M. Machino, S. Ito, Y. Kadoma and S. Fujisawa, *In Vivo*, 2012, **26**, 941-950.

38 S. Fujita and J. Taira, *Free Radic. Biol. Med.*, 1994, **17**, 273-277.

39 J. Taira, T. Ikemoto, K. Mimura, A. Hagi, A. Murakami and K. Makino, *Free Rad. Res. Comms*, 1993, **19**, S71-S77.

40 F. Bertrand, D.A. Basketter, D.W. Roberts and J.P. Lepoittevin, *Chem. Res. Toxicol.*, 1997, **10**, 335-343.

41 M. Lucarini, G.F. Pedulli, L. Valgimigli, R. Amorati and F. Minisci, *J. Org. Chem.* 2001, **66**, 5456-5462.

42 J.F. Arteaga, M. Ruiz-Montoya, A. Palma, G. Alonso-Garrido, S. Pintado and J.M. Rodríguez-Mellado, *Molecules*, 2012, **17**, 5126-5138.

43 A. Simić, D. Manojlović, D. Segan and M. Todorović, *Molecules*, 2007, **12**, 2327-2340.

Caption of Figures

Fig. 1. Schematic representation of a hydrogen peroxide (H_2O_2) permselective microsensor obtained by the electropolymerization of natural(-like) guaiacol derivatives (A) and drawing of a first-generation glucose biosensor made on top of the electrosynthesized poly-magnolol film (B). D-glucono-δ-Lactone (DGL); AA (ascorbic acid); DHAA (dehydroascorbic acid); DA (dopamine); DAQ (dopamine quinone); GOx (glucose oxidase); BSA (bovine serum albumin); GA (glutaraldehyde); Glu (glucose); PM (poly-magnolol); PSF (permselective film); E_{App} (applied potential *vs* Ag/AgCl).

Fig. 2. Cyclic voltammograms of eugenol (A), isoeugenol (B), dehydrodieugenol (C) and magnolol (D) on Pt-Ir in NaOH 0.1 M (100 mV/s). A progressive lowering of the current is visible from the first to the fifth scan for all the tested molecules, as well as the formation of non-conductive polymers on the electrode surface.

Fig. 3. Scanning electron microscope (SEM) at 5000 magnification for poly-eugenol, poly-

isoeugenol, poly-dehydrodieugenol and poly-magnolol electrodeposited onto Pt-Ir (I, J) in CV (A, C, E and G) and CPA (B, D, F and H) at day 1.

Fig. 4. *In vitro* calibration of glucose biosensor showing Michaelis-Menten kinetics and linear regression (inset).

Table 1. Cyclic voltammetry (CV) parameters and resulting oxidation peak potentials of the four phenols (monomers and dimers) used in this study in comparison with *o*PD. All the CV experiments were performed at room temperature by using freshly-made solutions (10 mM) and 20 mL electrochemical cell; the phenols were dissolved in 0.1 M NaOH (pH= 12.85) while *o*PD was dissolved in PBS (pH= 7.4). The lower and upper applied potentials (E_{App}) are referred to Ag/AgCl electrode.

Table 2. *In vitro* sensitivity characterization of new polymers in terms of linear slope, LOD and LOQ and permselectivity compared with PPD (n=4 for each group).